The General Dynamic Equation for Aerosols

Theory and Application to Aerosol Formation and Growth

FRED GELBARD AND JOHN H. SEINFELD

Department of Chemical Engineering, California Institute of Technology, Pasadena, California 91125

Received August 14, 1978; accepted September 11, 1978

Conservation equations for aerosol size distribution dynamics are derived and compared. A new discrete-continuous conservation equation is derived that overcomes the limitations of the purely discrete or continuous equations in simulating aerosol dynamics over a broad particle size spectrum. Several issues related to aerosol formation and growth not previously amenable to exact analysis are studied in detail using the discrete-continuous equation: (1) the establishment of a steady state concentration profile of molecular clusters in the presence of a preexisting aerosol; (2) the relative importance of nucleation, condensation, and scavenging in gas-to-particle conversion; and (3) the importance of cluster–cluster agglomeration relative to other processes. The formation and growth of a sulfuric acid/water aerosol in a smog chamber is simulated using the discrete-continuous equation, and the results are compared with recent experimental data. The above issues related to aerosol formation and growth are investigated for the simulated experiment.

INTRODUCTION

The dynamic behavior of an aerosol is described by a population balance equation. In its most general form the independent variables in the equation are particle size and composition (1), although in virtually all applications size is the only variable characterizing the aerosol. The population balance equation, which can be termed the general dynamic equation (GDE), can assume several forms depending on whether the aerosol size distribution is represented as discrete or continuous and on what physical and chemical phenomena are included. Because of the complex processes that an aerosol may undergo, simulation of the dynamics of an aerosol generally necessitates solution of some form of the GDE.

In the most fundamental approach to deriving the GDE, particles are represented as consisting of integer multiples of a single structural unit, typically a molecule. In these discrete equations particles differ only in the number of monomers they contain. The GDE consists then of an infinite set of nonlinear ordinary differential equations for the number densities of all particles. The discrete GDE, while rigorously valid, is impractical for simulation of aerosol behavior because of the typical wide range in particle size. A popular alternative to the discrete GDE is the continuous GDE, in which the particle size spectrum is taken to be continuous rather than discrete. Whereas the continuous GDE is more tractable than the discrete version, it suffers from the disadvantages of inaccurately representing processes occurring among the very smallest particles, processes that are important in representing gas-to-particle conversion.

The object of this work is to derive a new form of the aerosol GDE which we term the discrete-continuous GDE. In this form

0021-9797/79/020363-20$02.00/0

the discrete representation is used up to a certain multiplet number past which the particle size distribution is represented as continuous. The discrete-continuous GDE has the capability of representing the entire aerosol size distribution from single molecules to the largest particles, including all relevant physical phenomena occurring. A particular benefit of the discrete-continuous GDE is the ability to simulate for the first time the dynamics of molecular clusters in the presence of a preexisting aerosol. Because of this, the discrete-continuous GDE provides the opportunity to study theoretically a number of important questions related to aerosol formation and growth in reacting gas systems not previously amenable to exact analysis:

(1) Do the molecular clusters achieve a steady state and, if so, what are the relative concentrations of the particles and how large is the scavenging effect of a preexisting aerosol on the steady state concentrations?

(2) Can one estimate the relative importance of nucleation and condensation as routes for gas-to-particle conversion and will a particle burst be detected as a result of nucleation?

(3) How large is the error of neglecting cluster–cluster agglomeration?

Because in many cases the assumptions inherent in basic aerosol balance equations have not been clearly stated in the past, we hope additionally to clarify the limits of validity of commonly used aerosol equations.

We begin with the fundamental discrete representation of aerosol dynamics. Based on the discrete representation, the discrete-continuous GDE is derived. Next, the relationship between the discrete-continuous GDE and the common continuous GDE is elucidated. We conclude Part I of this work by using the discrete-continuous GDE to develop the theoretical framework needed to determine the relative importance of all physical processes, such as nucleation, condensation, and scavenging. Part II is devoted to a detailed application of the discrete-continuous GDE for simulating aerosol formation and growth in a reacting gas system. In the particular experiment simulated, the photochemical oxidation of SO_2 to sulfuric acid is taken as the primary aerosol-generating step. We predict the dynamic behavior of the sulfuric acid/water aerosol in the presence of a preexisting aerosol. In doing so, the above questions on aerosol formation and growth are addressed.

PART I. THEORETICAL DEVELOPMENT

In this section we derive the discrete-continuous GDE based on the rigorous discrete GDE. We then discuss general aspects of aerosol formation and growth.

Discrete General Dynamic Equation

We consider the following phenomena to be occurring: (1) agglomeration of two particles; (2) evaporation or escape of a monomer from a particle; and (3) homogeneous particle generation or removal processes apart from those that occur as a result of evaporation and agglomeration. As noted in the Introduction, we restrict our attention to size distribution dynamics and do not consider particle composition as an independent variable. Thus, the aerosol may be considered as chemically homogeneous for the purposes of deriving the governing dynamic equation.

For a spatially homogeneous aerosol the quantity of interest is the concentration of particles containing i monomers, where $i \geq 1$. Assuming an i-mer has a volume v_i, the concentration of i-mers, $N(v_i,t)$, will vary with time due to agglomeration, evaporation, generation, and removal processes. The rate of agglomeration of i-mers with j-mers is equal to the rate of formation of $(i + j)$-mers, and is given by

$$\frac{\beta(v_i,v_j)N(v_i,t)N(v_j,t)}{1 + \delta_{i,j}}, \quad i,j \geq 1 \qquad [1]$$

where $\delta_{i,j}$ is the Kronecker delta and $\beta(v_i,v_j)$ is the kinetic coefficient of agglomeration of two particles of volumes v_i and v_j. The functional form of $\beta(v_i,v_j)$ will be discussed later. If i is equal to j, we must divide by 2, so as not to count the agglomeration twice (2, 3, 4). The rate of evaporation of i-mers is

$$E(v_i)N(v_i,t), \quad i \geq 2 \qquad [2]$$

where $E(v_i)$ is the evaporation coefficient. The rate of formation of i-mers by agglomeration is the sum of all agglomerations resulting in an i-mer and is given by

$$\frac{1}{2}\sum_{j=1}^{i-1}\beta(v_{i-j},v_j)N(v_{i-j},t)N(v_j,t), \quad i \geq 2. \qquad [3]$$

The factor of one-half is introduced because β is a symmetric function of its arguments and therefore the summation counts each agglomeration twice for $i - j$ not equal to i. However, if i is an even integer, the term $\beta(v_{i/2},v_{i/2})N(v_{i/2},t)N(v_{i/2},t)$ is only counted once in the summation, but the factor of one-half is still required as given in Eq. [1]. The rate of depletion of i-mers by agglomeration with all other particles is given by,

$$N(v_i,t)\sum_{j=1}^{\infty}\beta(v_i,v_j)N(v_j,t), \quad i \geq 1. \qquad [4]$$

For j equal to i, the agglomeration rate is divided by 2 as given in Eq. [1], but because each agglomeration removes two i-mers, the rate is also multiplied by 2, thereby cancelling the factor of one-half. The rate of formation of i-mers by evaporation from $(i + 1)$-mers is

$$(1 + \delta_{1,i})E(v_{i+1})N(v_{i+1},t), \quad i \geq 1. \qquad [5]$$

For $i = 1$, the dissociation of a dimer leads to the formation of two monomers, therefore the Kronecker delta is used in Eq. [5]. The rate of depletion of i-mers due to evaporation is given by

$$E(v_i)N(v_i,t), \quad i \geq 2. \qquad [6]$$

Combining Eqs. [3]–[5] and [6] the net rate of formation of monomers is

$$\frac{dN(v_1,t)}{dt} = -N(v_1,t)\sum_{j=1}^{\infty}\beta(v_1,v_j)N(v_j,t) + \sum_{j=2}^{\infty}(1 + \delta_{2,j})E(v_j)N(v_j,t) + S_0(v_1,t) - S_1[v_1,t,N(v_1,t)] \qquad [7]$$

and the net rate of formation of i-mers for $i \geq 2$ is,

$$\frac{dN(v_i,t)}{dt} = \frac{1}{2}\sum_{j=1}^{i-1}\beta(v_{i-j},v_j)N(v_{i-j},t)N(v_j,t) - N(v_i,t)\sum_{j=1}^{\infty}\beta(v_i,v_j)N(v_j,t) + E(v_{i+1})N(v_{i+1},t) - E(v_i)N(v_i,t) + S_0(v_i,t) - S_1[v_i,t,N(v_i,t)] \qquad [8]$$

where S_0 and S_1 represent all homogeneous generation and removal processes, respectively. Combined with the appropriate initial conditions (i.e., $N(v_i,0)$, $i \geq 1$), Eqs. [7] and [8] constitute the discrete GDE for a spatially homogeneous aerosol. Because agglomeration constantly produces larger particles, Eqs. [7] and [8] are an infinite set of coupled ordinary differential equations.

Discrete-Continuous GDE

Although the discrete GDE is an accurate description of aerosol dynamics, the number of equations needed to simulate actual aerosols can be immense. For large particles the difference in size between an i-mer and an $(i + 1)$-mer is relatively small. Thus, for particles that contain $k + 1$ or more monomers, where $k \gg 1$, the discrete concentrations can be represented by $n(v,t)$,

which is a continuous function in the limit as $v_1/v_k \to 0$, defined by

$$N(v_i,t) = \int_{v_i-v_1/2}^{v_i+v_1/2} n(v,t)dv, \quad i \geq k+1. \quad [9]$$

We now divide the distribution into two regimes. For particle volumes smaller than or equal to v_k the discrete representation is used, and for particle volumes greater than or equal to v_{k+1} a continuous representation is used. Using Eq. [9], Eq. [7] becomes

$$\frac{dN(v_1,t)}{dt} = -N(v_1,t)\left[\sum_{j=1}^{k} \beta(v_1,v_j)N(v_j,t) + \int_{v_{k+1}-v_1/2}^{\infty} \beta(v_1,v)n(v,t)dv\right] + \sum_{j=2}^{k}(1+\delta_{2,j})E(v_j)N(v_j,t) + \int_{v_{k+1}-v_1/2}^{\infty} E(v)n(v,t)dv + S_0(v_1,t) - S_1[v_1,t,N(v_1,t)], \quad [10]$$

and for $2 \leq i \leq k$, Eq. [8] becomes

$$\frac{dN(v_i,t)}{dt} = \frac{1}{2}\sum_{j=1}^{i-1} \beta(v_{i-j},v_j)N(v_{i-j},t)N(v_j,t) - N(v_i,t)\left[\sum_{j=1}^{k}\beta(v_i,v_j)N(v_j,t) + \int_{v_{k+1}-v_1/2}^{\infty} \beta(v_i,v)n(v,t)dv\right] + \begin{cases} E(v_{i+1})N(v_{i+1},t), & 2 \leq i \leq k-1 \\ \int_{v_{k+1}-v_1/2}^{v_{k+1}+v_1/2} E(v)n(v,t)dv, & i = k \end{cases} - E(v_i)N(v_i,t) + S_0(v_i,t) - S_1[v_i,t,N(v_i,t)]. \quad [11]$$

To derive the governing equation for $n(v,t)$ in the continuous regime, substitute $n(v,t)dv$ for $N(v,t)$ in Eq. [8], for $v \geq v_{k+1} - v_1/2$. Assuming conservation of volume, such that $v_j = jv_1$, for $v_{k+1} \leq v_i \leq v_{2k}$,

$$\frac{d[n(v_i,t)dv]}{dt} = \sum_{j=1}^{i-k-1} \beta(v_i - v_j, v_j)N(v_j,t)n(v_i - v_j, t)dv \qquad i \geq k+2$$

$$+ \frac{1}{2}\sum_{j=i-k}^{k} \beta(v_i - v_j, v_j)N(v_i - v_j, t)N(v_j,t)$$

$$- n(v_i,t)dv\left[\sum_{j=1}^{k} \beta(v_i,v_j)N(v_j,t) + \int_{v_{k+1}-v_1/2}^{\infty} \beta(v_i,u)n(u,t)du\right] + E(v_i+v_1)n(v_i+v_1,t)dv - E(v_i)n(v_i,t)dv + S_0(v_i,t) - S_1'[v_i,t,n(v_i,t)]. \quad [12]$$

For $v > v_{2k} + v_1/2$,

$$\frac{d[n(v,t)dv]}{dt}$$

$$= \sum_{j=1}^{k} \beta(v - v_j, v_j)N(v_j,t)n(v - v_j, t)dv + \frac{1}{2}\int_{v_{k+1}-v_1/2}^{v-v_{k+1}+v_1/2} \beta(v - u, u)n(v - u, t)d(v - u)n(u,t)du - \sum_{j=1}^{k} \beta(v,v_j)N(v_j,t)n(v,t)dv$$

$$- n(v,t)dv \int_{v_{k+1}-v_1/2}^{\infty} \beta(v,u)n(u,t)du + E(v + v_1)n(v + v_1, t)dv - E(v)n(v,t)dv + S_0(v,t) - S_1'[v,t,n(v,t)], \quad [13]$$

where

$$S_1'[v,t,n(v,t)] = S_1[v,t,N(v,t)]. \quad [14]$$

Note that the Jacobian for the transformation from $(v - u, u)$ coordinates to (v,u) coordinates is unity, and therefore $du\, d(v - u) = dudv$ in the first integral on the right-hand side of Eq. [13]. Substituting this expression into Eq. [13] and dividing both Eqs. [12] and [13] by dv results in

$$\frac{dn(v_i,t)}{dt}$$

$$= \sum_{j=1}^{i-k-1} \beta(v_i - v_j, v_j)N(v_j,t)n(v_i - v_j, t) \qquad i \geq k + 2$$

$$+ \frac{1}{2}\sum_{j=i-k}^{k} \frac{\beta(v_i - v_j, v_j)N(v_i - v_j, t)N(v_j,t)}{v_1} - n(v_i,t)\left[\sum_{j=1}^{k} \beta(v_i,v_j)N(v_j,t) + \int_{v_{k+1}-v_1/2}^{\infty} \beta(v_i,u)n(u,t)du\right] + E(v_i + v_1)n(v_i + v_1, t) - E(v_i)n(v_i,t)$$

$$+ \bar{S}_0(v_i,t) - \bar{S}_1[v_i,t,n(v_i,t)] \quad [15]$$

for $v_{k+1} \leq v_i \leq v_{2k}$, $\bar{S}_0 = S_0/v_1$, and $\bar{S}_1 = S_1'/v_1$. For $v > v_{2k} + v_1/2$

$$\frac{\partial n(v,t)}{\partial t}$$

$$= \sum_{j=1}^{k} \beta(v - v_j, v_j)N(v_j,t)n(v - v_j, t) + \frac{1}{2}\int_{v_{k+1}-v_1/2}^{v-v_{k+1}+v_1/2} \beta(v - u, u)n(v - u, t)n(u,t)du - n(v,t)\sum_{j=1}^{k} \beta(v,v_j)N(v_j,t)$$

$$- n(v,t)\int_{v_{k+1}-v_1/2}^{\infty} \beta(v,u)n(u,t)du + E(v + v_1)n(v + v_1, t) - E(v)n(v,t) + \bar{S}_0(v,t) - \bar{S}_1[v,t,n(v,t)]. \quad [16]$$

Because agglomeration of two particles from the discrete regime can only introduce new particles in the continuous regime smaller than or equal to v_{2k}, the continuous regime is divided into two sections. The first section contains particles of volume v, where $v_{k+1} - v_1/2 \leq v \leq v_{2k} + v_1/2$, and the second section contains particles larger than $v_{2k} + v_1/2$. In the first section $n(v,t)$ is governed by Eq. [15], which is at most a system of k equations. Note that the second term of Eq. [16] is evaluated only for $v \geq 2v_{k+1} - v_1/2$. Combined with the appropriate initial conditions, Eqs. [10], [11], [15], and [16] constitute the discrete-continuous GDE.

Continuous GDE

If $N(v_i,t)$ is neglected for $2 \leq i \leq k$, Eqs. [15] and [16] become

$$\frac{\partial n(v,t)}{\partial t} = \frac{1}{2}\int_{v_{k+1}-v_1/2}^{v-v_{k+1}+v_1/2} \beta(v-u,u)n(v-u,t)n(u,t)du - n(v,t)\int_{v_{k+1}-v_1/2}^{\infty} \beta(v,u)n(u,t)du + \bar{S}_0(v,t) - \bar{S}_1[v,t,n(v,t)] + n(v-v_1,t)\beta(v-v_1,v_1)N(v_1,t) - n(v,t)[\beta(v,v_1)N(v_1,t) + E(v)] + E(v+v_1)n(v+v_1,t). \quad [17]$$

In the limit as $v_1/v \to 0$, the last three terms of Eq. [17] reduce to

$$-\frac{\partial}{\partial v}\{[\beta(v,v_1)N(v_1,t) - E(v)]v_1 n(v,t)\} + \frac{\partial^2}{\partial v^2}\left\{[\beta(v,v_1)N(v_1,t) + E(v)]\frac{v_1^2 n(v,t)}{2}\right\}. \quad [18]$$

For most aerosols it has been shown (5) that the second term of [18] can be neglected. Therefore Eq. [17] becomes

$$\frac{\partial n(v,t)}{\partial t} = \frac{1}{2}\int_{v_{k+1}-v_1/2}^{v-v_{k+1}+v_1/2} \beta(v-u,u)n(v-u,t)n(u,t)du - n(v,t)\int_{v_{k+1}-v_1/2}^{\infty} \beta(v,u)n(u,t)du + \bar{S}_0(v,t) - \bar{S}_1[v,t,n(v,t)] - \frac{\partial[I(v,t)n(v,t)]}{\partial v} \quad [19]$$

where $I(v,t) = [\beta(v,v_1)N(v_1,t) - E(v)]v_1$. As shown elsewhere (5), $I(v,t)$ is the net growth rate of a particle of volume v due to condensation and evaporation of monomers, and is commonly called the condensation growth rate or the growth law (6–9). Notice that Eq. [19] is defined only over the domain $v \geq v_{k+1} - v_1/2$, and all information on the distribution below this size is lost. One usually resorts to nucleation theory (10–12) to provide the generation rate of particles at $v = v_{k+1}$, thus supplying the boundary condition for Eq. [19]. A detailed discussion of the boundary condition will be given later.

Notice that the first integral on the right-hand side of Eq. [19] is not evaluated in the region $[v_{k+1} - v_1/2,\ 2v_{k+1} - v_1/2]$. This is because agglomerations that form new particles in this region are neglected, (except for the agglomeration of monomers with k-mers, which is accounted for in the boundary condition.)

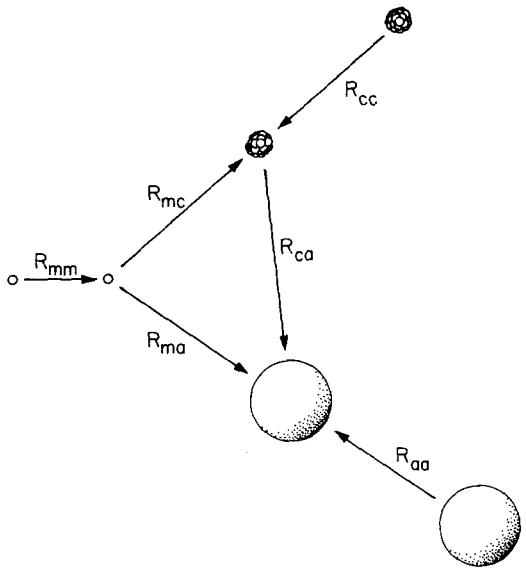

FIG. 1. Routes for gas-to-particle conversion. R_{ij} is the net agglomeration rate of particle type i with particle type j where m is monomer, c is cluster, and a is aerosol.

General Aspects of Aerosol Formation and Growth

A major current problem in atmospheric science is developing a fundamental understanding of the dynamic behavior of air pollution aerosols. The qualitative picture of polluted tropospheric aerosols that has emerged is that primary aerosols, both natural and anthropogenic, provide the surface upon which secondary species ultimately condense. The principal source of secondary aerosol constituents is the primary gaseous pollutants, such as SO_2, NO_x and hydrocarbons. A major route for formation of secondary aerosol species is conversion of primary pollutant species to secondary gaseous species, followed by condensation of the secondary vapors on existing particles or nucleation to form fresh particles. It is still under debate whether nucleation or condensation is the dominant mechanism for gas-to-particle conversion in the atmosphere. One can supposedly measure the flux of particles into the detectable size range of an instrument. However, the observed flux can be the result of the growth of small *preexisting* particles initially below the detectable limit or by the growth of particles formed by nucleation. Since current instrumentation (13, 14) is probably not capable of detecting a typical critical size particle, measurements from which the two mechanisms can be distinguished are virtually unavailable.

Because we wish to be precise in our definitions of condensation and nucleation as routes for gas-to-particle conversion, we will define clusters as particles containing i monomers, where $2 \leq i \leq k$, and aerosol particles as particles containing $k + 1$ or more monomers. In developing the discrete-continuous GDE, the only constraint on k is that it be a large number. Thus, one can consider a k-mer to be the critical size particle for nucleation or that just below the lower size limit of detection. In either case the discrete-continuous GDE can be used to determine the net rate of formation of particles smaller and larger than a k-mer. Thus, condensation will be defined as the net agglomeration rate of monomer and clusters with aerosol particles. Nucleation will be defined as the net formation rate of aerosol particles by the agglomeration of two clusters or a monomer with a k-mer. Classical nucleation is then a special case of nucleation, in which the k-mer is the critical size particle. (Classical nucleation theory neglects cluster-cluster agglomeration in determining the nucleation rate.) When we speak of the scavenging of an i-mer by a j-mer, we mean the net agglomeration rate of the two particles where $j \gg i$.

The general aspects of the gas-to-particle conversion process are depicted in Fig. 1. Monomer, the secondary gaseous species, may either condense on aerosol particles or agglomerate with another monomer to enter the path involving molecular cluster dynamics. The molecular clusters may themselves be scavenged by aerosol particles or continue to grow to the point at which an aerosol particle is formed, the nucleation

route. It is of interest to be able to estimate the relative importance of the two gas-to-particle conversion paths, direct condensation and nucleation, as a function of the generation rate of monomer and the quantity and size distribution of preexisting aerosol. In fact, there are several questions that arise in considering the general gas-to-particle conversion process:

(1) Is a steady state concentration profile of molecular clusters achieved, and, if so, how does the profile differ in the absence and presence of a preexisting aerosol?

(2) Can the relative importances of condensation, nucleation, and scavenging be estimated to determine the qualitative evolution of the aerosol, given knowledge of the monomer generation rate and the quantity and size distribution of preexisting aerosol?

(3) What is the importance of cluster–cluster agglomeration relative to the other processes influencing the cluster concentrations and the evolving aerosol size distribution?

The discrete-continuous GDE implicitly accounts for all the processes referred to in these questions, and, on that basis, its solution provides quantitative answers to them. In this section the theoretical analysis needed to address these questions for general gas-to-particle conversion systems will be presented. Subsequently, the analysis developed in this section will be used to answer the above questions for the particular experiment simulated.

For the six agglomeration processes (1) monomer–monomer (mm), (2) monomer–clusters (mc), (3) monomer–aerosol (ma), (4) cluster–aerosol (ca), (5) cluster–cluster (cc), and (6) aerosol–aerosol (aa), shown in Fig. 1, the net rate of agglomeration of particle types i and j, R_{ij} is,

$$R_{\mathrm{mm}} = \frac{1}{2}\beta(v_1,v_1)[N(v_1,t)]^2 - E(v_2)N(v_2,t), \quad [20]$$

$$R_{\mathrm{mc}} = \beta(v_1,v_2)N(v_1,t)N(v_2,t) - \int_{v_{k+1}-v_1/2}^{v_{k+1}+v_1/2} E(v)n(v,t)dv + \sum_{j=3}^{k} [\beta(v_1,v_j)N(v_1,t) - E(v_j)]N(v_j,t), \quad [21]$$

$$R_{\mathrm{ma}} = \int_{v_{k+1}-v_1/2}^{\infty} [\beta(u,v_1)N(v_1,t)n(u,t) - E(u + v_1)n(u + v_1, t)]du, \quad [22]$$

$$R_{\mathrm{ca}} = \sum_{j=2}^{k} N(v_j,t) \int_{v_{k+1}-v_1/2}^{\infty} \beta(v_j,u)n(u,t)du, \quad [23]$$

$$R_{\mathrm{cc}} = \frac{1}{2}\sum_{j=2}^{k}\sum_{j=2}^{k} \beta(v_i,v_j)N(v_i,t)N(v_j,t), \quad [24]$$

$$R_{\mathrm{aa}} = \frac{1}{2}\int_{v_{k+1}-v_1/2}^{\infty} \int_{v_{k+1}-v_1/2}^{\infty} \beta(v,u)n(u,t)n(v,t)dudv. \quad [25]$$

The net nucleation rate is,

$$R_{\mathrm{nuc}} = \sum_{i=k+1}^{2k} \left\{\frac{1}{2}\sum_{j=i-k}^{k} \beta(v_i - v_j, v_j)N(v_i - v_j, t)N(v_j,t)\right\} - \int_{v_{k+1}-v_1/2}^{v_{k+1}+v_1/2} E(u)n(u,t)du. \quad [26]$$

If a k-mer corresponds to the critical size particle, then R_{nuc} is the classical nucleation

rate, generalized to include cluster-cluster agglomeration. The net nucleation rate divided by the net condensation rate of particles in the discrete regime is

$$\xi = \frac{R_{\text{nuc}}}{R_{\text{ma}} + R_{\text{ca}}}. \qquad [27]$$

If $\xi \ll 1$ and $\xi \gg 1$, condensation and nucleation, respectively, are the dominant mechanisms.

It is also of interest to determine the net number of monomers nucleating, given by

$$R_{\text{m-nuc}} = \sum_{i=k+1}^{2k} \frac{i}{2} \{ \sum_{j=i-k}^{k} \beta(v_i - v_j, v_j) N(v_i - v_j, t) N(v_j, t) \} - (k+1) \int_{v_{k+1}-v_1/2}^{v_{k+1}+v_1/2} E(u) n(u,t) du. \qquad [28]$$

The net number of monomers from the discrete regime condensing on aerosol particles is

$$R_{\text{m-cond}} = \sum_{j=1}^{k} jN(v_j,t) \int_{v_{k+1}-v_1/2}^{\infty} \beta(v_j,u) n(u,t) du - \int_{v_{k+1}+v_1/2}^{\infty} E(u) n(u,t) du. \qquad [29]$$

Thus the fraction of the total flux of monomer entering the continuous regime by condensation is

$$\alpha = \frac{R_{\text{m-cond}}}{R_{\text{m-nuc}} + R_{\text{m-cond}}}. \qquad [30]$$

Although the nucleation rate may be comparable to the monomer and cluster condensation rate, due to the scavenging of the small aerosol particles, no significant particle formation may be observed just above the detection limit. Since it has been experimentally observed (15, 16), and theoretically predicted in this work, that after a short time lag a burst of new particles should form just above the detection limit, it is also important to determine if such a phenomenon will occur in general. Because nucleation can only introduce new particles of size v_i, where $k + 1 \leq i \leq 2k$, for a burst of new particles to be detected $dn(v_i,t)/dt$ must be positive as given by Eq. [15] for some $k + 1 \leq i \leq 2k$, $t \geq 0$, and a detectable limit of v_{k+1}.

Techniques for obtaining a priori estimates of the rates discussed in this section will be presented in the analysis of the experimental simulation.

II. APPLICATION OF THE DISCRETE-CONTINUOUS GDE TO AEROSOL SIZE DISTRIBUTION DYNAMICS IN A SMOG CHAMBER

In the study of gaseous air pollutants, chemical reactions are isolated from transport processes by carrying out atmospheric chemical reactions in laboratory vessels, commonly referred to as smog chambers. Chemical mechanisms derived from analysis of the results of smog chamber experiments are then employed, together with descriptions of transport and diffusion, to produce mathematical models of atmospheric gaseous pollutant behavior. As in the study of gas phase air pollution chemistry, smog chambers have also been employed to elucidate aerosol formation and growth in an environment free of the complications of transport and diffusion. A key step in the process of developing a comprehensive mathematical model for atmospheric aerosols is careful analysis of the results of smog chamber experiments in which aerosol formation and growth accompanies the usual gaseous chemistry. These experiments must be analyzed to test our understanding of the gas-

to-particle conversion process, to study the competition between condensation on existing particles and nucleation to form new particles, and to assess the importance of scavenging. A complication inherent in the performance and analysis of such experiments, not present in purely gaseous experiments, is that particle formation and growth is strongly influenced by the presence of existing aerosol. Thus, the initial conditions of aerosol number, size, and chemical composition in the reactor may substantially influence the ultimate quantity and size distribution of aerosol achieved. Experiments of this type are ordinarily carried out with an initial charge that is either particle-free or consists of particles characteristic of primary sources or ambient air.

The discrete-continuous GDE is ideally suited for the simulation of aerosol formation and growth in smog chambers, and this section is devoted to the first simulation of actual experimental aerosol data in such a situation. Of all the existing smog chamber experiments involving aerosols, the photochemical oxidation of SO_2 to form a sulfate aerosol is the most common. Although several experimental investigations have been reported (15–22), the mechanisms by which the aerosol develops are not completely understood. Aerosol formation from SO_2 has been simulated previously using the continuous GDE (23, 24). However, as previously discussed, the discrete-continuous GDE provides a more detailed description of the aerosol and does not rely on nucleation theory to describe the molecular cluster dynamics. Because of the recent availability of experimental data (22), we are also able to make direct comparisons of the predicted and measured aerosol number and volume distributions for photochemical oxidation of SO_2.

Description of the Experiment

We have chosen to simulate one of the experiments of McMurry (22), a recent and comprehensive study of aerosol formation from the photochemical oxidation of SO_2. In the experiment, a large Teflon bag was filled with unfiltered ambient air, doped with measured amounts of NO, NO_2, SO_2, and C_3H_6, and exposed to solar radiation throughout the filling and data acquisition period. Based on the initial SO_2 concentration of 81 ppb, the initial bag volume was computed to be 49 m^3 (after correcting for the measured background SO_2 concentration of 15 ppb). Experiment P17 is simulated here because both the temperature and relative humidity remained almost constant at 37°C and 34%, respectively, throughout. The initial distribution was taken from the third reported size distribution, because it corresponded to the time that the observed SO_2 concentration began to decrease. Logarithmic interpolation was used to fit the initial size distribution, but due to instrument limitations the size distribution for particle diameters below 0.0133 μm was obtained by extrapolation. (The validity of the extrapolation will be discussed later.) Based on the initial curve fit, the total number, surface area, and volume of particles with diameters from 0.0133 to 1 μm are 1.65×10^5 cm^{-3}, 5.55×10^2 μm^2 cm^{-3}, and 1.02×10^1 μm^3 cm^{-3}, respectively. It was assumed that all the SO_2 converted produced molecular H_2SO_4. The average loss rate of SO_2 was used to compute a constant rate of H_2SO_4 generation of 4.84×10^7 molecules sec^{-1} cm^{-3}. (For comparison, in a different study of H_2SO_4/H_2O aerosol formation, a generation rate of 1.25×10^7 molecules sec^{-1} cm^{-3} was used (24).)

Physical Properties of a H_2SO_4/H_2O Aerosol Photochemically Generated in the Presence of a Preexisting Urban Aerosol

One of the major difficulties in simulating experimental data is determining the physical properties of the aerosol. In most cases, even if all the chemical constituents of the

aerosol have been identified, the necessary thermodynamic data are not available. One is always confronted with the problem of determining particle properties such as diameter, vapor pressure, evaporation rate, and surface tension for a particle containing only a few molecules. Clearly, certain bulk concepts are meaningless for clusters containing several molecules, and the validity of extrapolating bulk values to molecular clusters is questionable.

We are faced here, therefore, with the problem of assuming the physical properties of the aerosol generated in the experiments of McMurry. In nearly all photochemical oxidation studies of SO_2 the assumed product is H_2SO_4 (22, 24, 25). Due to the presence of water vapor, it is also assumed that the particles consist of H_2SO_4/H_2O droplets. Unfortunately in dealing with an urban atmosphere the matter is further complicated because the preexisting aerosol undoubtedly contains a complex mixture of salts and organics. We will assume that the only effect of the ambient aerosol and gaseous impurities is to reduce the H_2SO_4 vapor pressure over the droplets to the point that evaporation of H_2SO_4 can be neglected to a first approximation. The reduction in particle vapor pressures due to impurities has recently been observed (26). The validity of neglecting evaporation of sulfuric acid will be discussed later.

For the bulk phase H_2SO_4/H_2O system all the necessary thermodynamic data are available (27–30). Except for the particle diffusivity, all physical properties were based on the bulk values. To account for the variation of composition with particle size it was assumed that for a particle containing a fixed number of H_2SO_4 molecules the number of H_2O molecules in the particle is determined by thermodynamic equilibrium. Due to the much higher concentration of H_2O in the gas phase, this is a valid assumption (31, 32). As shown elsewhere (33–35), the free energy of formation of a particle as a function of the H_2SO_4 and H_2O

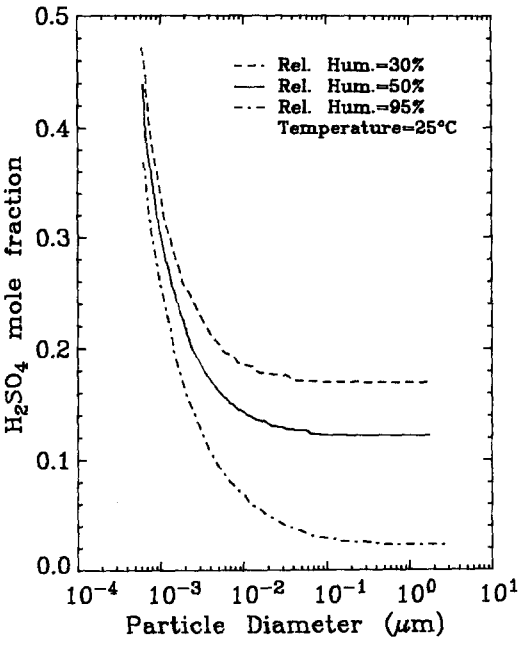

FIG. 2. Equilibrium concentration of H_2SO_4 in a spherical droplet of H_2SO_4 and H_2O, as a function of the relative humidity and particle diameter.

in the particle for a fixed temperature, H_2SO_4 gas phase concentration, and relative humidity can be computed. Since the free

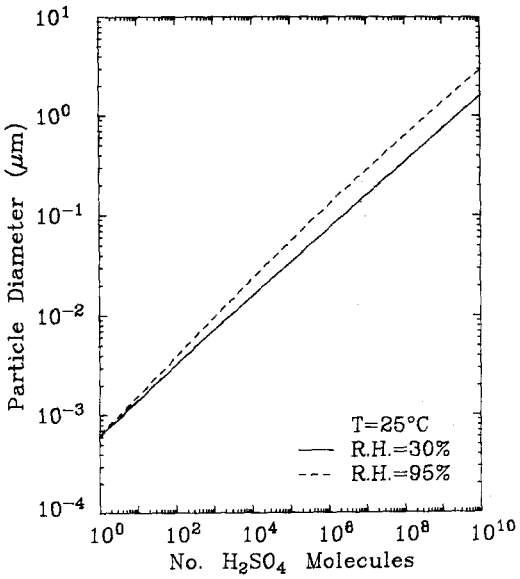

FIG. 3. Equilibrium particle size as a function of the relative humidity and the number of H_2SO_4 molecules in the particle.

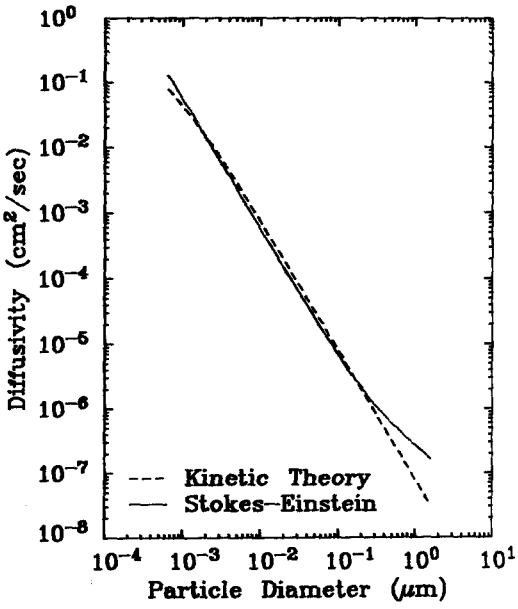

FIG. 4. Diffusivity for a H_2SO_4/H_2O particle at 37°C and 34% relative humidity. Particle composition and density as a function of size was determined by thermodynamic equilibrium.

energy surface is a saddle, there is a unique number of H_2O molecules associated with a fixed number of H_2SO_4 molecules for a minimum free energy of formation. Thus, for the conditions of the experiment, the particle density, surface tension, and acid concentration can be determined as a function of particle size. Because the operating temperatures of the experiment did not correspond to the temperature at which all the thermodynamic data are available, corrections were made to the thermodynamic data as described elsewhere (36).

It is interesting to note the variation of physical properties with particle size as determined on the basis of the above assumptions. As shown in Fig. 2, the H_2SO_4 mole fraction in the particle is highly dependent on the particle size and relative humidity. Also notice that for a fixed particle size, the H_2O concentration increases as the relative humidity increases. Therefore, Fig. 3 shows that due to the additional H_2O molecules the particle size increases for a fixed number of H_2SO_4 molecules in the particle, as the relative humidity increases.

To calculate the particle diffusivity, kinetic theory (37) can be used for molecules and smaller molecular clusters.[1] For larger particles the Stokes–Einstein expression (38) is more appropriate. Note from Fig. 4 that for the conditions of the experiment, at 37°C and 34% relative humidity, both expressions are not appreciably different over a wide range of particle diameters. Because the Stokes–Einstein expression (using Phillips' formula (39) for the drag), is considered valid for particles smaller than the mean free path of air (which is approximately 0.0714 μm at 37°C), the diffusivity for particle diameters larger than 0.00147 μm was calculated using the Stokes–Einstein expression, and for particle diameters smaller than 0.00147 μm by kinetic theory. As shown in Fig. 4, 0.00147 μm corresponds to the crossover point of the two expressions.

Simulation Results

The aerosol is assumed to consist of sulfuric acid–water particles in thermodynamic equilibrium at the temperature and relative humidity of the experiment. The quantity conserved during particle agglomeration is the number of sulfuric acid molecules. Thus, the independent variable v in the GDE will be the number of sulfuric acid molecules rather than the particle volume. Since particle size is uniquely related to the number of sulfuric acid molecules in the particle at any relative humidity, v can be converted to particle volume. The details of solving the GDE numerically are given elsewhere (40).[2] In the computations the Fuchs–Phillips agglomeration coefficient (41) was

[1] It should be noted that the diffusivity calculated from kinetic theory (37) is also an approximation.

[2] It is important to monitor the so-called "finite domain error," by checking that

$$\sum_{i=1}^{k} v_i N(v_i,t) + \int_{v_{k+1}-v_1/2}^{\infty} vn(v,t)dv$$

is conserved during the computation. For the present application v represents the number of H_2SO_4 molecules, and for the times and the domain considered the error was less than 0.4%.

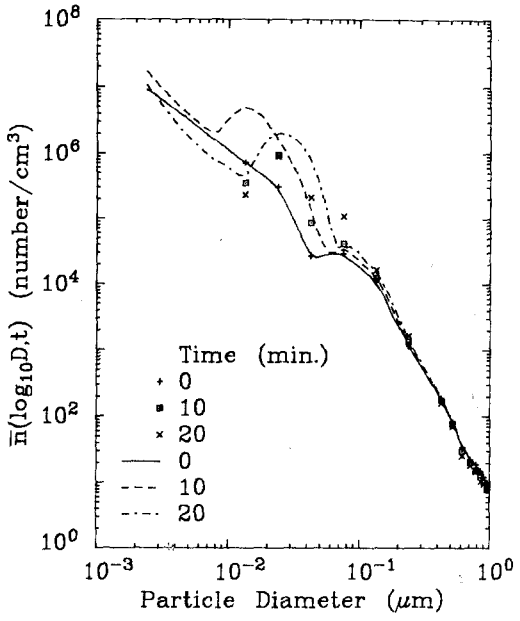

FIG. 5. Number distribution evolution. Discrete points are the measured values and the lines are the computed results. The initial distribution for particle diameters below 0.0133 μm was obtained by extrapolation.

used, and the upper limit on particle size was taken to be 1-μm diameter.

The computed and measured number distributions, in terms of $\bar{n}(\log D,t) = n(v,t)dv/d \log D$, are shown in Fig. 5. Agreement between the predicted and observed spectra below about 0.1-μm diameter is not as good as that above 0.1 μm. The discrepancy between predicted and observed size distributions in the lower end of the spectrum can be a result of the neglect of monomer evaporation from small particles or an inaccurate extrapolation of the initial size distribution into the nondetectable size regime. In addition, the accuracy of the data at the smallest particle sizes was estimated to be only within an order of magnitude (42). The actual evaporation rate probably lies somewhere between that of pure sulfuric acid/water and the assumed value of zero. Based on the assumption of no evaporation and each collision results in coalescence, the predicted number density represents that for a maximum particle growth rate. Another possible source of error arises in extrapolating the initial size distribution below the detectable limit down to the monomer. The particles below the detection limit grow by agglomeration and condensation, and may have a significant effect on the distribution in the detectable size range.

For large particles the errors committed by neglecting evaporation and extrapolating the initial distribution are smaller and thus better agreement between the predictions and the data is expected. The number distribution changes very little for large particles and comparisons are best made using the volume distribution $V(\log D,t)$, where $V(\log D,t) = \pi D^3 \bar{n}(\log D,t)/6$. Figure 6 shows that the predicted volume distribution agrees very well with the data for large particle sizes.

Establishment of the Steady State Molecular Cluster Profile in the Presence of a Preexisting Aerosol

A key assumption of classical nucleation theory is the existence of a steady state concentration profile of molecular clusters smaller than the critical size (10–12, 43). According to the classical theory, the scavenging effect of any preexisting aerosol, which would reduce the nucleation rate, is neglected. However, using the discrete-continuous GDE it can be shown that due to scavenging a steady state profile *different* from that predicted by classical nucleation theory is rapidly established in the presence of a preexisting aerosol.

Figure 7 shows the computed concentration profile in the discrete regime for the conditions of the experiment of McMurry (22) in which evaporation was neglected. The profile first rapidly increases due to the generation of H_2SO_4 monomer. As monomers and clusters agglomerate, larger cluster are formed, resulting in a rapid increase in the cluster profile. However, as larger particles are formed in the continuous regime, the scavenging of smaller particles increases

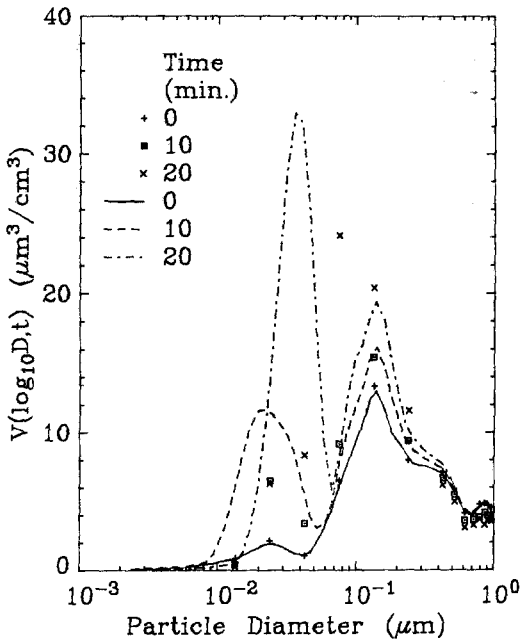

FIG. 6. Volume distribution evolution. Discrete points are the measured values, and the lines are the computed results.

and the discrete concentration profile gradually decreases as shown. It was found that after reducing the initial cluster profile by an order of magnitude, practically the same cluster profile was established within 1-min. Also, the choice of the initial cluster profile did not significantly affect the evolving discrete or continuous regimes. One can determine the time required to reach steady state as a function of cluster size by solving for the steady state profile and comparing it to the dynamically calculated profile. Based on this work, time scales on the order of minutes were probably required to reach steady state for the simulated experiment. (It should be noted, however, that we have not determined the exact time or largest cluster size for which the steady state approximation is valid.)

In the development of classical nucleation theory no account is made for the presence of particles much larger than the critical size. In the atmosphere, however, preexisting aerosol may have a significant effect on the nucleation rate. The preexisting aerosol serves as a condensation site for clusters and thus scavenges clusters before they reach the critical size for nucleation. If one neglects the scavenging effect, the resulting cluster profile is significantly higher, as shown in Fig. 8. (The lowest profile will be discussed later.) Hence the classical theory would predict an aerosol independent nucleation rate greater than the aerosol dependent nucleation rate with scavenging.

Determination of the Relative Importance of Condensation, Nucleation, and Scavenging for Gas-to-Particle Conversion

Having previously developed the general expressions for the rates of all processes, we would now like to apply the expressions in the analysis of the experiment just simulated. Unfortunately, in order to evaluate any of the rate expressions R_{ij}, the discrete-continuous GDE must be solved so that the distribution is known as a function of time. However, if one is interested only in a priori

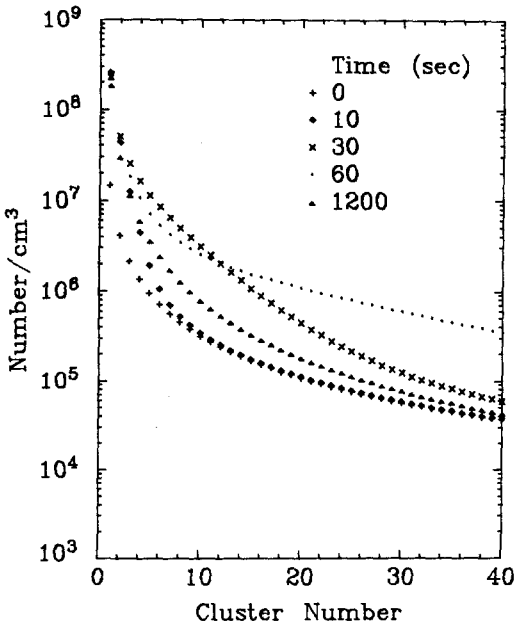

FIG. 7. Evolution of the concentration profile of molecular clusters in the discrete regime.

estimates, the steady state approximation can be used for the discrete regime as discussed in the previous section. Although the steady state profile changes as the aerosol evolves, the temporal variations are small and qualitatively predictable. As the aerosol grows, greater scavenging of the particles in the discrete regimes occurs. Thus, $N(v_i,t)$ for $1 \leq i \leq k$, will, in general, decrease after the steady state is established, as shown in Fig. 7.

The computed total number densities in the discrete and continuous regimes are shown as solid lines in Fig. 9 (the broken lines will be discussed later). During the first 30 sec, a large number of small particles are predicted to form in the discrete regime. After 30 sec these small clusters are predicted to nucleate at the boundary between the discrete and continuous regimes, and thus a burst of new particles occurs in the continuous regime. Since the 23.6-Å boundary between the two regimes is probably less than the present lower limit of detection

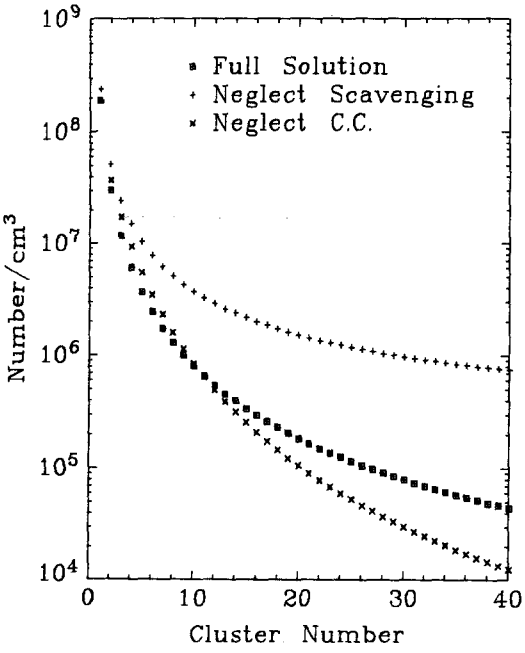

FIG. 8. Comparison of cluster concentration profiles in the discrete regime after 20 min of simulation (C.C. stands for cluster–cluster agglomeration.)

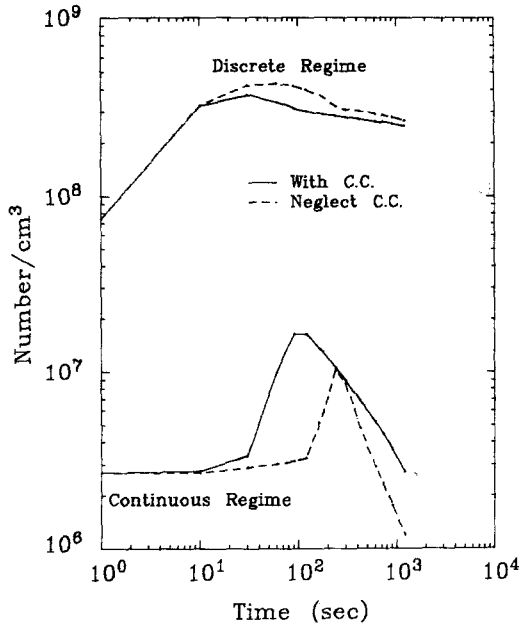

FIG. 9. Total number of particles/cm³ in the discrete and continuous regimes. The discrete regime is from 0.0006 to 0.00237-μm diameter and the continuous regime is from 0.00237 to 1.0-μm diameter. Broken lines calculated by neglecting cluster–cluster agglomeration.

of the condensation nuclei counter (14), it is clear why a time delay is often observed between the time of initiation of condensable species generation and the time of first aerosol detection. Time lags from 45 sec to several minutes have been reported (15, 16), although not all experiments have shown a significant time lag (18). After the particle burst, the newly formed particles in the continuous regime continued to grow, with the resulting wave formation in the distribution shown in Fig. 5.

In order to determine if a particle burst will occur in general, define $dn_0(v_i)/dt = dn(v_i,0)/dt$, and $dn_{ss}(v_i)/dt$ as the right-hand side of Eq. [15] based on the initial cluster profile and the steady state profile, respectively. Then if $dn_{ss}(v_i)/dt > 0$ a particle burst should occur. If $dn_{ss}(v_i)/dt < 0$ but $dn_0(v_i)/dt > 0$, a very short burst should occur but once the transients have decayed, scavenging will dominate and no significant

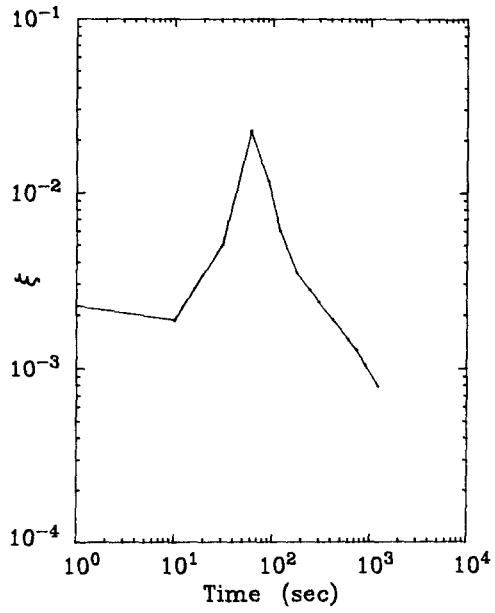

FIG. 10. Ratio of the nucleation rate to the condensation rate for the simulated experiment.

particle bursts should occur. (Clearly if $dn_0(v_i)/dt < 0$ and $dn_{ss}(v_i)/dt < 0$ no particle burst should occur.) One can also obtain an estimate of $n(v_{k+1} - v_1/2,t)$ by extrapolating the steady state profile to a $(k + 1)$-mer. Then if $n(v_{k+1} - v_1/2(2,t) = N(v_{k+1}, t)/v_1$, is much greater than $n(v_{k+1} - v_1/2,0)$, a particle burst may occur. To determine the movement of the wave in the distribution, as a result of condensational growth, the exact solution can be used (9).

In the experiment just simulated, R_{mm}, R_{mc}, R_{cc}, R_{nuc}, and R_{m-nuc} decreased after 1 min due to the increased scavenging resulting from aerosol growth. As shown in Fig. 10, $\xi \ll 1$; hence most of the monomer and clusters leave the discrete regime by condensation and not nucleation. Since there is a time lag from the initiation of monomer generation to nucleation, the initial accumulation of monomer and clusters results in a decrease in ξ, due to increased condensation. However, once the growing clusters pass into the continuous regime, ξ peaks, as shown in Fig. 10, and then continually decreases. Except for this short period, when the clusters enter the continuous regime, the dominant process for monomer conversion is condensation. Figure 11 shows that $\alpha > 0.9$ throughout most of the simulation, indicating that more than 90% of the monomer is converted to aerosol by condensation.

Determination of the Importance of Cluster-Cluster Agglomeration

A second key assumption of classical nucleation theory is neglect of the agglomeration of molecular clusters. The validity of such an approximation can now be evaluated.

Define $N'(v_i,t)$ as the discrete concentration of i-mers computed without cluster–cluster agglomeration. Then $\epsilon(v_i,t) = N'(v_i,t)/N(v_i,t)$ is an indication of the error committed in neglecting cluster–cluster agglomeration. If ϵ does not significantly differ from unity for $1 \leq i \leq k$, cluster–cluster agglomeration can be neg-

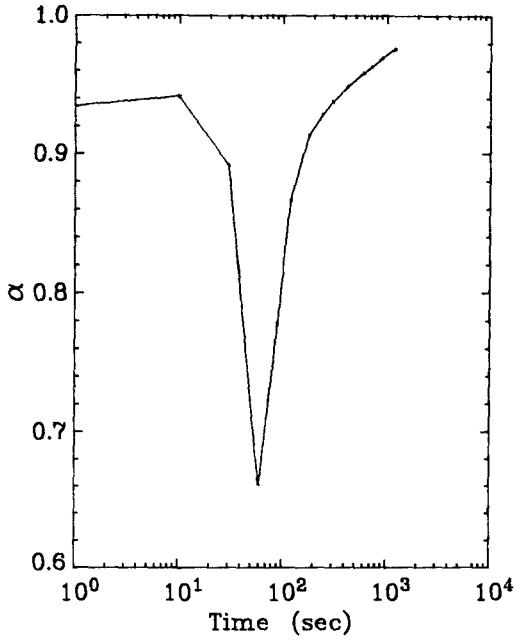

FIG. 11. Fraction of the total flux of monomer entering the continuous regime by condensation for the simulated experiment.

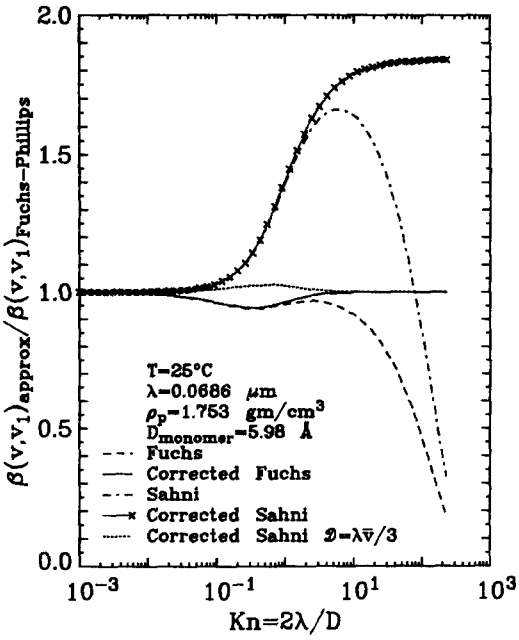

FIG. 12. Ratio of the agglomeration coefficient between a monomer of volume v_1, with a particle of volume v (assuming $v = \pi D^3/6$), calculated from existing growth laws divided by the Fuchs–Phillips agglomeration coefficient (41).

lected. In simulating McMurry's experiment, evaporation was neglected and ϵ was generally significantly different than unity for the clusters. Errors committed in the cluster concentrations introduce errors in the continuous regime, due to the nucleation of the clusters. Hence, Fig. 9 shows significant discrepancies for the total number of particles in the continuous regime computed with and without cluster–cluster agglomeration. Figure 8 also shows that significant errors in the profile result if cluster–cluster agglomerations are neglected. Thus cluster–cluster agglomeration apparently played an important role in the formation of new particles in the continuous regime. However, by neglecting cluster–cluster agglomeration, agreement was obtained with the full solution for large particles which grow primarily by condensation.

One can compute the steady state cluster concentrations if cluster–cluster agglomeration is negligible and evaporation is present, by iterating on the monomer concentration and solving a linear system of algebraic equations with a tridiagonal coefficient matrix. Although in the experiment simulated, both evaporation and cluster–cluster agglomeration cannot be neglected, if circumstances are such that both processes can be neglected, then McMurry (22) has shown that the cluster concentrations can be obtained directly.

Use of the Continuous GDE

Probably because of its simplicity, the solution to the continuous GDE is the approach usually taken to simulate aerosol dynamics. To apply the continuous GDE, $\beta(v, u)$, $I(v,t)$, and an initial and boundary condition must be specified. However, specifying the boundary condition on particle size makes application of the continuous GDE for simulating gas-to-particle conversion difficult, without first solving the discrete-continuous GDE. In this section the growth law and the boundary condition, which are unique to the continuous GDE, will be discussed.

The growth law, $I(v,t)$, is usually obtained from one of two interpolation formulas as given by Fuchs (44) or Sahni (45). (For convenience the curve fit of Fuchs and Sutugin (6) is used for Sahni's growth law.) As shown in (9), both formulas differ only in the assignment of three constants. Although these expressions are valid in the limits of Kn large and small, where the Knudsen number $Kn = 2\lambda/D$, difficulties arise when applying the formulas to situations in which the monomer is condensing on a particle not much larger than the monomer itself. The growth laws can be corrected for monomer condensation on an i-mer by multiplying the expressions by $[(1 + i^{1/3})/i^{1/3}]^2[(1 + i)/i]^{1/2}$ (46). With this correction, $I(v,t)/N(v_1,t)$ approaches $\beta(v,v_1)$ for $E(v) = 0$. Figure 12 shows $\beta(v,v_1)$ obtained from the growth law relative to the Fuchs–Phillips expression for Brownian coagulation.

Particle diffusivities were calculated based on kinetic theory for small particles and the Stokes–Einstein expression for large particles. The transition point between the two theories was chosen such that the diffusivity is a continuous function of particle size, as previously discussed. Notice that the approximate formulas greatly differ for large Kn without the correction factor. Also notice that even the corrected Sahni expression significantly differs from the Fuchs–Phillips coefficient unless the self-diffusion coefficient, $D = \lambda\bar{v}/3$ is used, where $\bar{v} = [8kT/\pi m]^{1/2}$, m is the monomer mass, T is the absolute temperature, and k is the Boltzmann constant.

To determine the boundary condition at $v = v_{k+1} - v_1/2$, we note that implicit in Eq. [9] is constancy of $n(v,t)$ in the regions $[v_{k+1} - v_1/2 + \ell v_1,\ v_{k+1} + v_1/2 + \ell v_1]$, where ℓ is a positive integer or zero. (Although $n(v,t)$ is actually a series of step functions, because the spacing of the steps is so small relative to v, $n(v,t)$ can be used as a continuous function.) Thus, at the boundary $n(v_{k+1} - v_1/2,\ t)$ is given by $N(v_{k+1},t)/v_1$. Using Eq. [15] and neglecting the clusters we have

$$\frac{dN(v_{k+1},t)}{dt} = J - E(v_{k+1})N(v_{k+1},t) - \beta(v_{k+1},v_1)N(v_{k+1},t)N(v_1,t) + E(v_{k+2})N(v_{k+2},t) - N(v_{k+1},t)\int_{v_{k+1}-v_1/2}^{\infty} \beta(v_{k+1},u)n(u,t)du \quad [43]$$

where J is equal to $\beta(v_1,v_k)N(v_1,t)N(v_k,t)$.

Dividing Eq. [43] by v_1 results in the boundary condition

$$\frac{dn(v_{k+1} - v_1/2,\ t)}{dt} = \frac{J}{v_1} - n(v_{k+1},t)[E(v_{k+1}) + \beta(v_{k+1},v_1)N(v_1,t)] + E(v_{k+2})n(v_{k+2},t) - n(v_{k+1},t)\int_{v_{k+1}-v_1/2}^{\infty} \beta(v_{k+1},u)n(u,t)du. \quad [44]$$

There are, however, difficulties associated with determining J and hence the boundary condition. As previously discussed, because of the scavenging by particles in the continuous regime, the discrete profile, and hence the nucleation rate is dependent on the continuous distribution. Therefore, if the profile in the discrete regime is affected by scavenging, J will vary as the continuous regime evolves and *cannot* be determined in the absence of knowledge of the dynamics in the continuous regime.

By using a boundary condition for the continuous GDE obtained from the solution to the discrete-continuous GDE, it was found that the two solutions agreed. Furthermore, the exact condensation solution (9) agreed with the discrete-continuous solution for particles above 0.1-μm diameter. However, because aerosol–aerosol agglomeration is neglected in the exact condensation solution, the predicted distribution was larger than the full solution for particle diameters below 0.1 μm.

SUMMARY AND CONCLUSIONS

A new form of the general dynamic equation (GDE) for aerosols, termed the discrete-continuous GDE, has been developed. The strength of the equation lies in the ability to simulate aerosol dynamics in systems in which processes are occurring over a broad particle size spectrum, such as aerosol formation and growth in reacting gas systems. Whereas the most fundamen-

tal, the discrete GDE is impractical for simulating aerosol processes involving more than a few hundred particle sizes. The continuous GDE is capable, in principle, of representing aerosol dynamics over the complete particle size spectrum, although, in practice, the dynamics of molecular clusters are not adequately represented by this equation. In addition, problems arise in properly specifying the boundary condition on the continuous GDE at the lower end of the size spectrum when fresh particles are being formed by gas-to-particle conversion. The desire to simulate aerosol dynamics in systems in which fresh particles are being formed from reacting gases in the presence of a preexisting aerosol, the typical urban atmospheric situation, in fact, prompted the present work. Previous attempts to simulate this situation have been based on the use of the continuous GDE together with classical nucleation theory to specify the flux of fresh, stable particles into the system. We have shown here that classical nucleation theory, however, may be inaccurate in predicting the flux of stable nuclei in this system, since the theory neglects the scavenging of molecular clusters by aerosol particles.

With the discrete-continuous GDE it is now possible to simulate the detailed processes occurring during aerosol formation and growth in reacting gas systems. We have simulated the dynamics of sulfuric acid/water aerosols generated by photochemical oxidation of sulfur dioxide in a smog chamber in the presence of a preexisting aerosol, since this system has been one of the most frequently studied, and experimental data of McMurry are available (22). Agreement between predictions and data were generally good, although uncertainties in the system, such as the exact composition of the aerosol and the complete initial distribution, precluded precise, quantitative comparisons. More importantly, we have been able to study for the first time two long-standing and important issues related to aerosol behavior in gas-to-particle conversion: (1) the establishment of a steady state concentration profile of molecular clusters in both the presence and absence of a preexisting aerosol and (2) the relative roles of condensation, nucleation, and cluster–cluster agglomeration in transferring mass to the larger particles in the spectrum. In particular, we found that a steady state profile is established for the molecular clusters and that under certain circumstances the profiles differ in the absence and presence of a preexisting aerosol and cluster–cluster agglomeration can be important relative to other processes influencing molecular clusters. Finally, dimensionless criteria were developed to estimate the relative importance of nucleation, condensation, and cluster–cluster agglomeration for general gas-to-particle conversion processes.

ACKNOWLEDGMENTS

This work was supported by National Science Foundation grant ENV76-04179. The authors wish to thank Dr. Peter H. McMurry for furnishing the experimental data and discussing the experimental procedure.

REFERENCES

1. Chu, K. J., and Seinfeld, J. H., *Atmos. Environ.* **9**, 375 (1975).
2. Chapman, S., and Cowling, T. G., "The Mathematical Theory of Non-Uniform Gases," p. 91. Cambridge Univ. Press, New York, 1964.
3. Fuchs, N. A., "The Mechanics of Aerosols," p. 290. Pergamon, New York, 1964.
4. Hidy, G. M., and Brock, J. R., "The Dynamics of Aerocolloidal Systems," pp. 298–299. Pergamon, Oxford, 1970.
5. Ramabhadran, T. E., Peterson, T. W., and Seinfeld, J. H., *A.I.Ch.E.J.* **22**, 840 (1976).
6. Fuchs, N. A., and Sutugin, A. G., *in* "Topics in Current Aerosol Research" (Hidy, G. M., and Brock, J. R., Eds.), Vol. 2, pp. 29–37. Pergamon, Oxford, 1971.
7. Heisler, S. L., and Friedlander, S. K., *Atmos. Environ.* **11**, 156 (1977).
8. Peterson, T. W., Ph.D. Thesis, Calif. Inst. Tech. 1977.
9. Gelbard, F., and Seinfeld, J. H., Exact solution of

the general dynamic equation for aerosol growth by condensation, *J. Colloid Interface Sci.* **68,** 173 (1979).
10. Frenkel, J., "Kinetic Theory of Liquids," pp. 366–413. Dover, New York, 1955.
11. Zettlemoyer, A. C. (Ed.), "Nucleation." Marcel Dekker, New York, 1969.
12. Abraham, F. F., "Homogeneous Nucleation Theory." Academic, New York, 1974.
13. Thermo Systems Inc., Operating and Service Manual, Model 3030 Electrical Aerosol Analyzer, 500 Carigan Road, St. Paul, Minn. 55112.
14. Instrument Instruction Manual for Condensation Nuclei Monitor, Model Rich 100, Environment One Corp., 2773 Balltown Road, Schenectady, N.Y. Also see, Liu, B. Y. H., and Kim, C. S., *Atmos. Environ.* **11,** 1097 (1977).
15. Evans, G. R., and Roddy, A. F., "Proc. 7-th Int'l. Conf. Condensation and Ice Nuclei, Prague and Vienna," p. 369. 1969.
16. Luria, M., Olszyna, K. J., De Pena, R. G., and Heicklen, J., *J. Aerosol Sci.* **5,** 435 (1974).
17. Haury, G., Jordan, S., and Hofman, C., *Atmos. Environ.* **12,** 281 (1978).
18. Cox, R. A., and Penkett, S. A., *J. Chem. Soc. Faraday Trans.* **68,** 1735 (1972).
19. Friend, J. P., Leifer, R., and Trichon, M., *J. Atmos. Sci.* **30,** 465 (1973).
20. Bricard, J., Cabane, M., Madelaine, G., and Vigla, D., *J. Colloid Interface Sci.* **39,** 42 (1972).
21. Cox, R. A., *J. Aerosol Sci.* **4,** 473 (1973).
22. McMurry, P. H., Ph.D. Thesis, Calif. Inst. Tech. 1977.
23. Wadden, R. A., Quon, J. E., and Hulburt, H. M., *Atmos. Environ.* **8,** 1009 (1974).
24. Kiang, C. S., and Middleton, P., *Geophys. Res. Lett.* **4,** 17 (1977).
25. Hamill, P., Kiang, C. S., and Cadle, R. D., *J. Atmos. Sci.* **34,** 150 (1977).
26. Chang, D. P. Y., and Hill, R. C., "Retardation of Aqueous Droplet Evaporation by Air Pollutants," presented at 71st Annual Air Pollution Control Ass. Meeting, Houston, TX, June 1978.
27. Sebinina, L., and Terpugow, L., *Z. Phys. Chem. A* **173,** 237 (1935).
28. Giauque, W. F., Hornung, E. W., Kunzler, J. E., and Rubin, T. R., *J. Amer. Chem. Soc.* **82,** 62 (1960).
29. Gmitro, J. I., and Vermeulen, T., "Vapor-Liquid Equilibria for Aqueous Sulfuric Acid," UCRL-10886 (1963).
30. Perry, R. H., and Chilton, C. H. (Eds.), "Chemical Engineers Handbook," 5th ed., pp. 3–80, 81. McGraw–Hill, New York, 1973.
31. Hamill, P., *J. Aerosol Sci.* **6,** 475 (1975).
32. Hamill, P., Toon, O. B., and Kiang, C. S., *J. Atmos. Sci.* **34,** 1104 (1977).
33. Reiss, H., *J. Chem. Phys.* **18,** 840 (1950).
34. Doyle, G. J., *J. Chem. Phys.* **35,** 795 (1961).
35. Mirabel, P., and Katz, J. L., *J. Chem. Phys.* **60,** 1138 (1974).
36. Itoh, M., Takahashi, K., and Kasahara, M., *J. Aerosol Sci.* **8,** 183 (1977).
37. Kennard, E. H., "Kinetic Theory of Gases," pp. 195–196. McGraw–Hill, New York, 1938.
38. Friedlander, S. K., "Smoke, Dust and Haze," pp. 27–31. Wiley, New York, 1977.
39. Phillips, W. F., *Phys. Fluids* **18,** 1089 (1975).
40. Gelbard, F., and Seinfeld, J. H., Numerical solution of the dynamic equation for particulate systems, *J. Comp. Phys.* **28,** 357 (1978).
41. Sitarski, M., and Seinfeld, J. H., *J. Colloid Interface Sci.* **61,** 261 (1977).
42. McMurry, P. H., private communication.
43. Katz, J. L., *J. Chem. Phys.* **52,** 4733 (1970).
44. Fuchs, N. A., "Evaporation and Droplet Growth in Gaseous Media," p. 8. Pergamon, Oxford, 1959.
45. Sahni, D. C., *J. Nucl. Eng. A/B* **20,** 915 (1966).
46. Friedlander, S. K., *Phys. Fluids* **3,** 693 (1960).